Snow heterogeneous reactivity of bromide with ozone lost during snow metamorphism.

Jacinta Edebeli[1,2], Jürg C. Trachsel[3], Sven E. Avak[1], Markus Ammann[1], Martin Schneebeli[3], Anja Eichler[1,4], Thorsten Bartels-Rausch[1]

[1]Laboratory of Environmental Chemistry, Paul Scherrer Institut, Villigen PSI, Switzerland
[2]Swiss Federal Institute of Technology, ETH Zurich, Zürich, Switzerland
[3]WSL-Institute for Snow and Avalanche Research SLF, Davos Dorf, Switzerland
[4]Oeschger Centre for Climate Change Research, University of Bern, Bern, Switzerland

Correspondence to: Thorsten Bartels-Rausch (thorsten.bartels-rausch@psi.ch)

Abstract. Earth's snow cover is very dynamic on diurnal time scales. The changes to the snow structure during this metamorphism have wide ranging impacts such as on avalanche formation and on the capacity of surface snow to exchange trace gases with the atmosphere. Here, we investigate the influence of dry metamorphism, which involves fluxes of water vapor, on the chemical reactivity of bromide in the snow. For this, the heterogeneous reactive loss of ozone in the dark at a concentration of 5-6$\times 10^{12}$ molecule cm^{-3} is investigated in artificial, shock-frozen snow samples doped with 6.2 µM sodium bromide and with varying metamorphism history. The oxidation of bromide in snow is one reaction initiating polar bromine releases and ozone depletions. We find that the heterogeneous reactivity of bromide is completely absent from the air-ice interface in snow after 12 days of temperature gradient metamorphism and suggest that burial of non-volatile bromide salts occurs when the snow matrix is restructuring during metamorphism. Impacts on polar atmospheric chemistry are discussed.

1 Introduction

Snow on Earth hosts chemical reactions that impact the composition of the atmosphere (Dominé and Shepson, 2002; Grannas et al., 2013). One example is the oxidation of bromide and the subsequent release of bromine from arctic snow (Abbatt et al., 2010; Saiz-Lopez and von Glasow, 2012). This reactive halogen species participates in ozone destroying chemical cycles in the gas phase. Ozone is one of the main oxidants in the lower atmosphere with impact on atmospheric composition, health, and climate (Simpson et al., 2007). Recent improvement in global atmospheric chemistry models indicate that halogen chemistry accounts for about 14% of the global tropospheric ozone sinks (Schmidt et al., 2016). In addition, the reactive halogen species are potent oxidants for organics and, of particular interest, gas phase mercury (Simpson et al., 2007; Simpson et al., 2015). Oxidized mercury partitions readily into condensed phases from where it may enter the ocean and the food-web upon seasonal snow melt (Steffen et al., 2008).

Dominé et al. (2008) argued that the efficient chemical reactivity in snow is linked to its physical properties. Snow is a porous matrix that is dense enough to provide a large surface area for heterogeneous reactions, but not too dense to limit transport and light penetration as seen in soil, for example. The heterogeneous oxidation of bromide by ozone, a potential pathway for bromine release both in the dark and in sunlight (Abbatt et al., 2010), has been shown to be very efficient on ice and brine surfaces (Wren et al., 2010; Oldridge and Abbatt, 2011; Edebeli et al., 2019). The high rates on aqueous solutions have been linked to an ozonide intermediate and its stabilisation at the surface (Artiglia et al., 2017). Taken that the bromide needs to be accessible to gas-phase ozone for an efficient heterogenous oxidation, the location of these chemical reactant - its distribution between the air-ice interface and other reservoirs in the interior of the snow - is a key determinant for their chemical reactivity (Bartels-Rausch et al., 2014; Hullar and Anastasio, 2016; McFall et al., 2018). Field studies have revealed a high heterogeneity in bromine release and bromide concentration in snow and have attributed this heterogeneity to the initial source of bromide and to post-depositional changes of the location (Jacobi et al., 2012; Pratt et al., 2013).

One prominent post-depositional mechanism is dry metamorphism shaping the structure and physical properties of snow with impact on heat transfer, albedo, and avalanche formation (Blackford, 2007; Dominé et al., 2008; Schweizer, 2014). Snow at Earth's surface that is exposed to varying temperature gradients with time undergoes continued sublimation and deposition during metamorphism with complete re-building of the entire snow matrix every few days (Pinzer et al., 2012). Earth's snow cover can be exposed to temperature gradients between 10 °C m^{-1} to 100 °C m^{-1} (Birkeland et al., 1998). Dominé et al. (2015) showed that such temperature gradient conditions can prevail on a seasonal scale: in low-arctic tundra, snow is exposed to a temperature gradient mostly above 20 °C m^{-1} between mid-November and early February. The consequences are changes in the isotopic composition of the snow with implications for ice core dating (Steen-Larsen et al., 2013; Steen-Larsen et al., 2014; Ebner et al., 2017). Further, Hagenmuller et al. (2019) observed dust particles being incorporated into the ice matrix of snow driven by the intensive water vapor fluxes during dry, temperature gradient metamorphism.

With the turnover of snow grains and the movement of water vapor, contaminants may be redistributed between the surface and bulk of the snow grains: Studies investigating the adsorption and uptake of trace gases such as nitric acid and hydrochloric acid with growing ice have observed higher uptake than in ice at equilibrium (Kärcher and Basko, 2004; Ullerstam and Abbatt, 2005; Kippenberger et al., 2019). Kippenberger et al. (2019) has shown that the burial of volatile acids is a strong function of acidity, growth rate, and temperature. At equilibrium, adsorption of acidic trace gases leads to the acids or their anions entering the ice phase at considerable concentration only within the interfacial region of a few nm depth, as recently observed for hydrochloric acid and volatile organic acids (Krepelova et al., 2013; Bartels-Rausch et al., 2017; Kong et al., 2017; Waldner et al., 2018).

Therefore, recrystallization in snow might have a significant impact on the fraction of contaminants or reactants located at the air-ice interface of snow and thus on the heterogeneous chemistry of ions in snow. Laboratory studies investigating temperature

gradient metamorphism effects in natural and artificial snow have observed a strong influence of metamorphism on the elution behaviour of ions such as ammonium, fluoride, chloride, calcium and sulphate. Whereas calcium and sulphate were found to be enriched at the air-ice or ice-ice interface during snow metamorphism, ammonium, fluoride, and chloride were buried in the bulk of the snow (Hewitt et al., 1989, 1991; Cragin et al., 1996; Trachsel et al., 2019).

Here, we study the effect of sublimation and growth of ice during snow metamorphism on bromide reactivity in well controlled laboratory experiments. The sodium bromide used in this study is non-volatile and field studies have related its mobility in the snowpack to its vivid photochemical transformation into volatile bromine. Bromine is released to the air and may re-deposit on the snow surface after formation of stickier bromine compounds (Toom-Sauntry and Barrie, 2002). The objective of this study is to investigate the heterogeneous reactivity of bromide oxidation by gas-phase ozone in the dark. To assess the surface concentration of bromide and its change during temperature gradient metamorphism the gas-phase ozone loss is monitored in this study. Bromide concentration in the doped snow samples (6.2 μM) is typical for snow on Arctic sea ice (Pratt et al., 2013).

Experimental

Snow samples were prepared by shock-freezing aqueous solutions (Bartels-Rausch et al., 2004; Trachsel et al., 2019) and stored in a metamorphism box with a well-defined temperature gradient at the WSL Institute for Snow and Avalanche Research SLF in Davos (Trachsel et al., 2019). After the exposure to the temperature gradient, the structurally intact individual samples were exposed to ozone in a packed-bed flow tube set-up to derive the impact on the reactivity with gas-phase ozone (Bartels-Rausch et al., 2004). The structure of snow samples before and after metamorphism was imaged by X-ray microtomography (Trachsel et al., 2019).

Sample preparation

Artificial snow was produced by spraying and shock freezing droplets of a sample solution in liquid nitrogen using a homebuilt sprayer (Bartels-Rausch et al., 2004; Trachsel et al., 2019). The samples were left overnight at –45°C and then, stored isothermally at –5 °C for 7 days to anneal and to minimize internal grain-boundaries (Blackford, 2007; Riche et al., 2012). The samples were returned to - 45 °C after this isothermal treatment to slow down further changes with time and stored up to 54 days at - 45 °C prior to the metamorphism experiments to reach a quasi-steady-state. The snow was sieved using pre-cleaned stainless-steel sieves (Retsch, Germany) in a –20°C cold laboratory at the WSL Swiss Snow and Avalanche research Institute (SLF, Davos, Switzerland). Snow grains in the size range 300 – 600 μm were packed into the 12.0 ± 0.1 cm long glass reactor tubes with 2.4 ± 0.1 cm internal diameter.

The sample solution was either ultrapure water (18 MΩ quality, arium pro, Sartorius, Göttingen, Germany) (undoped snow) or an aqueous sodium bromide (NaBr, Sigma Aldrich, >99.0%) solution in ultrapure water (doped snow). The bromide

concentration in the sieved snow crystals was 6.2±0.18 μM (498 ± 14 ppbw) in the doped snow and <0.12 μM (<10 ppb) in the undoped snow as determined by ion chromatography (Metrohm (Herisau, Switzerland) 850 Professional IC, 872 Extension Module, 858 Professional Sample Processor autosampler). A Metrosep A Supp 10 column (Metrohm) was used and the eluents were a 1.5 mM Na_2CO_3 and 0.3 mM $NaHCO_3$ in a 1:1 mixture followed by 8 mM Na_2CO_3 and 1.7 mM $NaHCO_3$ in a 1:1 mixture with a flow rate of 0.9 cm^3 min^{-1}. Possible instrumental drifts were monitored by measuring a standard after every 20^{th} sample.

Metamorphism

For the temperature gradient metamorphism experiments, samples were exposed to a gradient of 31 °C m^{-1} for 12 days in a snow metamorphism box mounted in a cold room at –8 °C (at SLF, Davos, Switzerland). The metamorphism box was a heavily insulated box with a heating plate set to –4 °C at the bottom. Over this plate, there was a ~ 2-3 cm thick layer of ice from ultrapure water. The sample holders were mounted on a disk with a 0.5 cm layer of ice made with ultrapure water in contact with the snow grains to increase thermal contact (Pinzer and Schneebeli, 2009). The spaces between the sample tubes were filled by sieving in snow. The box was then covered with a thin plastic film in contact with the filled-in snow and caps of the samples to avoid losses due to sublimation. This set-up resulted in an effective temperature at the bottom and at the top of the snow samples of -4.4 ± 0.1 °C and -8.1 ± 0.1 °C, respectively.

After the temperature gradient metamorphism treatment, the samples were stored at –45°C. For comparison, additional samples were stored isothermally at -20 °C at SLF, Davos, Switzerland for 12 days. In total, 12 samples were prepared from the homogenized snow batches: 2 undoped and 2 doped samples that experienced 12-days temperature gradient metamorphism, 2 undoped and 2 doped samples without temperature gradient metamorphism, 2 undoped and 2 doped samples that experienced iso-thermal metamorphism. Two replica samples – those of the doped snow that was exposed to temperature metamorphism for 12 days and the replica of the undoped snow that was not exposed to temperature gradient metamorphism - could not be analysed due to technical failures during the experiments.

Structural changes in the samples were assessed using an X-ray computer micro-tomography scanner (Scanco micro-CT 40) with a resolution of 10 μm. This microCT was operated at –20°C. Details of operations of the microCT scans have been described by Pinzer and Schneebeli (2009). The reconstructed microCT images were filtered with a Gaussian filter (support 2 voxels, standard deviation 1 voxel) and the threshold for segmentation was applied according to Hagenmuller et al. (2014). Structural parameters of the segmented ice structure were extracted with the software tools of the microCT device (Image Processing Language, Scanco Medical) to calculate the porosity and specific surface area.

Packed bed flow tube experiments

Samples were exposed to ozone at –15°C. Before exposure, about 2 cm of the samples were scraped off from the top and bottom of the samples to avoid potential contamination from contact with the ice layer on the disk in the metamorphism box or the caps for the sample holder/reactor tubes. An exception to this is one of the 0-day doped samples where 3 cm were shaved off. Afterwards, the mass of each snow sample during the ozone exposure was determined based on the weight of the filled and empty sample tube. The sample tubes were placed in the reactor cell, an insulated cooling jacket, at –15°C. The sample was allowed to temperature equilibrate for an hour before exposure to gases. Humidified airflow of ~200 cm^3 min^{-1} O_2 and ~200 cm^3 min^{-1} N_2 was delivered through the sample for 30 minutes to condition the sample. The total flow rate through the sample was set between 339 cm^3 min^{-1} to 352 cm^3 min^{-1} at norm temperature and pressure of 273.15 K and 1013.25 bar. This airflow was humidified to a water vapor pressure of ice at –15.0 ± 0.3 °C.

Ozone was generated by passing the N_2/O_2 airflow through a pen ray Hg UV lamp. The ozone flow was also humidified before delivery to the sample. The ozone flow was alternated between a bypass and the sample to control for drifts in ozone concentration. Ozone concentration was monitored using a commercial analyser (Teledyne, model 400E). The average ozone concentration for each experiment was slightly different due to the day to day variability in the efficiency of the ozone generator. For all experiments, ozone concentrations varied from 163 to 212 ppb ($4.7\text{-}6.2\times10^{12}$ molecule cm^{-3}). The maximum variability during any one experiment was less than 5 ppb after attaining initial stability at the start of the experiment. This drift was accounted for during analysis using fitting routines.

To confirm perfect flow conditions in the packed bed flow tubes, the chromatographic retention of acetone was determined for some samples at -30°C. Once the ozone experiment was finished, the samples were exposed to a flow of acetone in humidified N_2 (Bartels-Rausch et al., 2004). The observed retention time of acetone at -30°C matched calculations based on the air-ice partitioning coefficient (Dominé and Rey-Hanot, 2002; Winkler et al., 2002; Peybernes et al., 2004; Bartels-Rausch et al., 2005; Crowley et al., 2010) and the specific surface area of the snow sample as derived by microCT measurements for the undoped and doped samples after temperature gradient metamorphism.

1 Results and Discussion

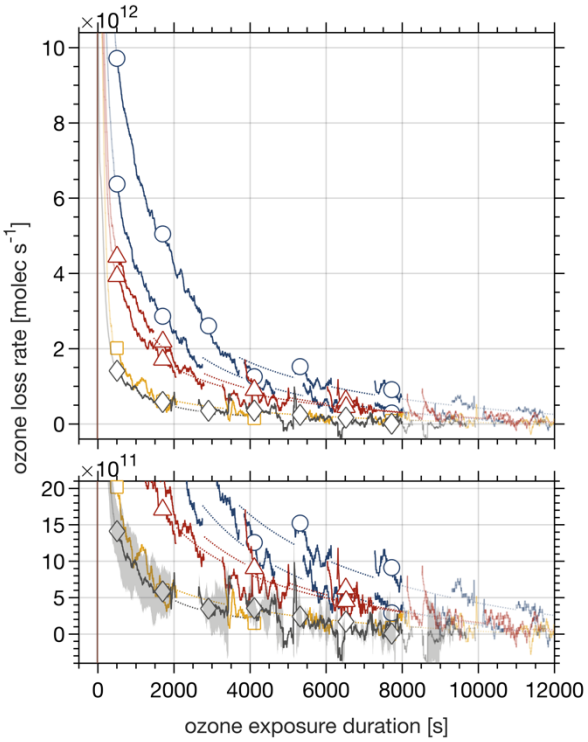

Figure 1: Ozone loss rate with duration of exposure. The snow samples with a bromide concentration of 6.2 µM experienced 0 days (blue lines, open circles) and 12 days (yellow line, open squares) of metamorphism with a temperature gradient of 31 °C m^{-1}. The lower panel is a zoom to the data. Ozone data were recorded continuously (lines), the markers are guides. The dotted lines are guide to the eyes, for periods where ozone loss data are not available (see text for details). Also shown are the ozone loss rates of snow samples after 12 days of isothermal metamorphism at -20 °C (red lines, open triangles). The grey line (open diamonds) denotes the average ozone loss rates of 5 samples with no bromide added and with and without exposure to temperature gradient metamorphism. The shaded area in the lower panel shows the standard deviation. The gas phase mixing ratio of ozone varied between 4.7-6.2×10^{12} molecule cm^{-3} for individual samples. Temperature during ozone exposure was -15 °C. At time 0, ozone in the carrier gas was passed over the snow samples.

Figure 1 shows ozone loss rates for snow samples prior to and after exposure to dry metamorphism. The ozone loss rate was derived based on observed changes in gas-phase ozone concentration downstream of the flow tube packed with the snow sample. The ozone loss curves can be classified into three regions:

1. All samples show a high (> 9×10^{12} molecule s^{-1}) loss rate during the initial period of ozone exposure up to 500 s. This observed loss is attributed to the reaction of ozone with traces of impurities, to a delay by switching the gas flows, and to the residence time of the ozone gas in the porous snow and is not further analysed.

2. In the intermediate time regime from about 500 s to 8000 s, the ozone loss rate is largest for the two samples doped with 6.2 μM bromide prior to ageing under laboratory-controlled temperature gradient metamorphism with 4×10^{12} molecule s^{-1} and 7×10^{12} molecule s^{-1} at 1000 s duration of ozone exposure (Fig. 1, blue lines, open circles). The loss rate was reduced by a factor of about 4 - 7 in the snow sample that experienced temperature gradient metamorphism with 1×10^{12} molecules s^{-1} at 1000 s duration of ozone exposure (Fig 1, yellow line, open square). This loss rate is indistinguishable from that in the samples without added bromide with a mean of 1×10^{12} molecule s^{-1} and with a standard deviation of 0.4×10^{12} molecules s^{-1} at 1000 s for 5 samples (Fig. 1, grey line, open diamonds).

   Also shown is the loss rate from 2 samples that experienced isothermal metamorphism for 12 days at -20 °C (Fig. 1, red lines, open triangles). The loss rate is only slightly reduced compared to the samples before exposure to metamorphism strongly supporting the driving role of the temperature gradient.
3. After about 8000 s ozone exposure, the ozone loss rates of all experiments approach zero loss of ozone. The raw data curves levelled off approaching a steady loss rate of $1.1\text{-}1.9\times10^{12}$ molecule s^{-1}. This background loss rate may be attributed to the reactive uptake of ozone to ice driven by a self-reaction on the ice surface (Langenberg and Schurath, 1999), which is the main phase in the frozen solution samples investigated here. Langenberg and Schurath (1999) described a reactive ozone uptake coefficient on ice of $7.7\text{-}8.6\times10^{-9}$ at -15 °C and at ozone gas-phase concentrations similar to our work. The uptake coefficient normalizes the loss rate to the collision rate of ozone with the ice (or snow) surface. A loss rate of $0.86\text{-}0.90\times10^{12}$ molecules s^{-1} can be derived based on the reported uptake coefficient for the experimental conditions of our doped samples prior to metamorphism, in good agreement with our observations. Because this loss rate is not related to the bromide in the samples, it has been subtracted from the data discussed and shown in Fig. 1.

Ozone loss compared to previous work

The reaction of gas-phase ozone with frozen solutions containing bromide has been studied in great detail previously (Wren et al., 2010; Oldridge and Abbatt, 2011; Abbatt et al., 2012; Wren et al., 2013). Oldridge and Abbatt (2011) described coated wall flow tube studies on frozen sodium bromide/sodium chloride/water mixtures at -15°C and Wren et al. (2010) reported on a laser-induced fluorescence study with sodium bromide/water mixtures at - 20°C. The studies by Wren et al. (2010) and by Oldridge and Abbatt (2011) were done with an initial sodium bromide concentration of 10 mM and a gas-phase ozone concentration of 1×10^{14} molecule cm^{-3} and 80×10^{14} molecule cm^{-3}, respectively. Oldridge and Abbatt (2011) have argued that this multiphase reaction proceeds in the liquid fraction of sample containing bromide-brine that is in equilibrium with ice between 0 °C and the eutectic temperature where the salt precipitates. The eutectic temperature of sodium bromide is at or below -28 °C (Stephen and Stephen, 1963).

The concentration of sodium bromide in the reactive solutions in equilibrium with ice is a sole function of temperature, and thus with a concentration of 3.4 M during the ozone exposure at -15° similar even for our samples that were frozen from aqueous solutions with 6.2 µM bromide. For this calculation, the freezing point depression data by Stephen and Stephen (1963); Rumble (2019) was used.

Despite the differences in the concentration of bromide in the solutions used to freeze the films, the similar concentration of bromide in the brine during ozone exposure makes a comparison of the experimental results feasible. For the comparison, the reported uptake coefficients of 1.5×10^{-8} and $4\text{-}2\times10^{-8}$, respectively (Wren et al., 2010; Oldridge and Abbatt, 2011), were transferred into loss rates based on the specific surface area of the snow sample used in this work and an ozone concentration of $4.7\text{-}6.2\times10^{12}$ molecule cm^{-3}. The loss rate prior to temperature gradient metamorphism found in the work presented here agrees with loss rates of $2\text{-}6\times10^{12}$ molecule s^{-1} as derived based on these earlier experimental works. Uncertainty in this comparison comes from the very low ozone concentration of 5×10^{12} molecule cm^{-3} used in the study presented here. Based on the results by Oldridge and Abbatt (2011), one would expect increasing surface reaction rates with lower ozone concentrations. Further, the surface coverage and the volume of the reactive sodium bromide brine at the interface might vary significantly due to the differences in sample geometries and in sample preparation. Please note that in this work, we refrain from discussing the results as uptake coefficient, as generally only the specific surface area of the snow is known, but not that of the reactive brine.

Location of impurities

The striking loss of heterogeneous reactivity during temperature gradient metamorphism raises the question of the location of the reactive bromide in the shock-frozen, artificial snow samples before metamorphism. Snow can host impurities in several compartments (Bartels-Rausch et al., 2014): Chemical species, besides water, and ions can be molecularly embedded within the ice matrix (solid-solution), molecularly adsorbed at the air-ice interface, in liquid or solid patches at the air-ice interface, in micropockets within the ice matrix including the ice-ice interface (at grain boundaries). Clearly, only bromide in direct contact with the gas phase, that is located at the air-ice interface or within the bulk at a distance that allows sufficient diffusion to the interface, is accessible to gas-phase ozone and thus reactive. In the following, we elaborate on the feasibility of bromide being hosted in these distinct departments in the samples used here.

Shock freezing aqueous solutions may preserve the homogeneous distribution of solutes also in the ice matrix from where the bromide might diffuse to the air-ice interface and heterogeneously react with the ozone. In the following, this reacto-diffusive loss is estimated. Due to lack of knowledge of the diffusion coefficient of bromide in ice, the diffusion coefficient of HNO_3 in crystalline ice at -15 °C of 100×10^{-12} cm^2 s^{-1} (Thibert and Dominé, 1998) was used as upper limit and a diffusion coefficient of HCl at -15 °C of 3×10^{-12} cm^2 s^{-1} as lower bound was used in this calculation. Further, the aqueous concentration of 6.2 µM and the specific surface area of each snow sample as derived by the microCT data (Table 1) was used. Based on these

assumptions, one may estimate that the total amount of bromide diffusing from the ice bulk to the surface is 0.2 - 1.6×10^{10} molecules each second. This is much less than the ozone loss observed in our experiments, clearly showing that the bromide is not present homogeneously in the ice matrix of the snow samples after shock freezing.

Exclusion of bromide to the ice-air interface during freezing has been observed by others at higher concentration (Wren et al., 2010). We find exclusion of bromide from the rapidly growing ice during shock-freezing even though the aqueous concentration is significantly lower than the typical solubility limits for ions in ice (details below), which might also be related to kinetic effects during fast ice growth. Thibert and Dominé (1997, 1998) derived solubilities of up to 0.1 mM to 1 mM for HCl and up to 0.06 mM to 0.6 mM for HNO_3 in ice at -8 °C to -35 °C, respectively. These data describe the equilibrium between gas-phase acid and solid solution and may serve as estimate for the solubility limit of sodium bromide in ice. Even though it is thus very likely that the ice might hold 6.2 µM of bromide as solid solution (total amount of bromide divided by the total ice volume), the measured ozone loss rates indicate that sufficient amounts of bromide to form brine are excluded to the ice-air interface after shock freezing.

We propose that the brine forms liquid patches on the surface and filaments along the grain boundaries at the interface as observed for higher concentrated frozen salt solutions (Blackford et al., 2007). A homogenous film covering the total snow surface is unlikely: A back-of-the-envelope calculation with the total amount of bromide doped to the samples and with a concentration of 3.4 M gives a brine layer with a thickness of only ~0.1 nm at -15°C for the specific surface area of the doped snow samples. This is unfeasible, because the thickness of an ice monolayer is roughly 0.3 nm. Whether the unreactive fraction of the bromide is located in a solid solution or in micropockets within the ice matrix is beyond the scope of this work, both compartments explain its non-reactivity.

Quantifying the bromide loss

Generally, the products and reaction mechanism of the bromide oxidation by ozone in the aqueous phase strongly depend on reaction time, reactant concentration and pH (Haag and Hoigne, 1983; Heeb et al., 2014). For non-acidified conditions, as in our study, hypobromous acid (HOBr/OBr^-) is the main product (R1) that may react further with ozone (R2) to form bromite (BrO_2^-), disproportionate to bromide (Br^-) and bromate (BrO_3^-), or self-react to dibromine monoxide (Br_2O) (Heeb et al., 2014). Despite uncertainties in the precise product distribution in this study, ozone is lost in our study in the initial reaction with bromide and to some extent in the subsequent oxidation of hypobromous acid to bromite resulting in 1-2 ozone molecules lost per bromide ion. In particular at acidic conditions as relevant for atmospheric waters and ices (Abbatt et al., 2012; Bartels-Rausch et al., 2014); bromine is formed and released to the atmosphere in a sequence of reaction steps (R1 and R3).

$Br^- + O_3 \longrightarrow OBr^- + O_2$ (R1)

$OBr^- + O_3 \longrightarrow BrO_2^- + O_2$ (R2)

$OBr^- + Br^- + H^+ \longrightarrow Br_2 + OH^-$ (R3)

Thus, assuming a net loss of 1 ozone molecule per bromide molecule, one might estimate about 0.9 and 1.7×10^{16} molecules of bromide are available for the multiphase reaction with ozone in the two porous snow samples prior to metamorphism. Assuming a net loss of 2 ozone molecules, 1.8 and 3.3×10^{16} molecules of available bromide can be estimated for the two samples. The cumulative loss was derived by integrating the area below the loss rate curves in Fig. 1 between 500 and 8000 s and subtracting the cumulative loss of the undoped sample to account for the presence of impurities also in the samples doped with bromide. For this analysis, the missing data in periods where the carrier gas was bypassing the snow to monitor the ozone concentration delivered to the flow tube were estimated using a power fit to the data (Figure 1). The cumulated amount of reacted bromide can be compared to the total amount of bromide of 4 and 6×10^{16} molecules initially added to the snow sample. Apparently, 22 % - 26 % and 44 % to 52 % in maximum of the bromide was accessible to gas-phase ozone prior to metamorphism.

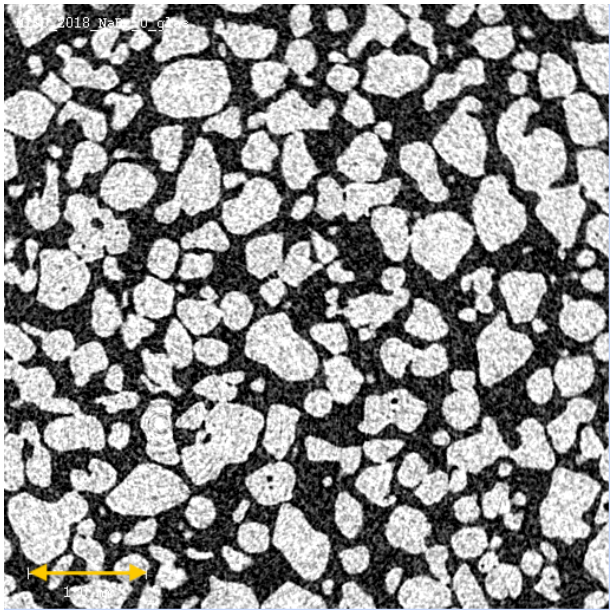

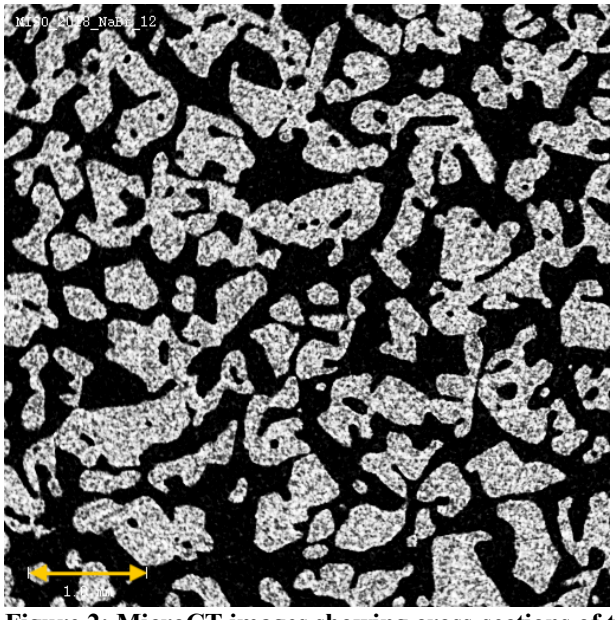

Figure 2: MicroCT images showing cross-sections of the doped snow samples after 0 days (upper) and 12 days (lower) exposure to temperature gradient metamorphism. White areas show the ice phase, black represents interstitial air. The scale bar (yellow arrow) denotes 1 mm.

Structural Changes to the snow.

Table 1 lists the physical properties of the snow samples. The specific surface area (SSA) and the porosity are within the range observed for hard wind-packed snow and depth hoar in the field (Legagneux et al., 2002; Zermatten et al., 2011; Calonne et

al., 2012). The structural changes to the snow during the 12 days temperature gradient metamorphism are visualised by X-ray microtomography (microCT) images in Fig. 2. In the microCT image of the snow sample prior to metamorphism individual spheres with 300 – 600 µm diameter are visible (Fig. 2, upper image). With developing snow metamorphism, the spheres get increasingly bonded and a new porous snow structure forms, while the recognition of the individual snow particles is lost (Fig. 2, lower image). This reconstruction is a direct consequence of the temperature gradient in snow resulting in water vapour pressure gradients which induce fluxes of water vapour from warmer to colder regions. In the experiments described here, the locally and continuously sublimating and growing snow, with an ice growth rate of 2 nm s^{-1} (Trachsel et al., 2019), leads to about 5 complete renewal cycles of the snow structure during the 12-days temperature gradient metamorphism (Pinzer et al., 2012). That changes in SSA do not necessarily reflect water turn-over rates during metamorphism has been discussed before (Pinzer et al., 2012). The samples that were stored isothermally at -5 °C for 7 days and up to 54 days at - 45 °C prior to the metamorphism experiments (Fig. 2 upper image), show also facets, as is typical for isothermal snow (Kämpfer et al., 2005; Löwe et al., 2011).

Table 1: Settings for the snow samples; The number of days gives the duration of metamorphism. Br denotes the concentration of bromide as derived by ion chromatography; SSA is the specific surface area as derived from the microCT scans with an typical error of ± 6% (Kerbrat et al., 2008). The density was derived based on the weight of the snow sample and the volume of the sample holder. The mass denotes the amount of snow during the ozone exposure experiments and the surface area denotes the total surface area of the snow during the ozone exposure experiments. Each experiment with added bromide and an average of the 5 experiments with no added bromide is shown in Figure 1 and discussed in this work.

	Br [µM]	SSA [cm g^{-1}]	density of snow [g cm^{-3}]	mass [g]	Surface area [cm^2]
0 days	6.2	183	0.33	17	3118
0 days	6.2	183	0.32	11	2018
12 days, 31 °C cm^{-1} gradient	6.2	162	0.41	14	2268
12 days, isothermal	6.2	143	0.45	16	2281
12 days, isothermal	6.2	143	0.35	14	1996
0 days	<0.12	195	0.35	13	2540
0 days	<0.12	195	0.3	10	1953
0 days	<0.12	176	0.3	12	2113
12 days, 31 °C cm^{-1} gradient	<0.12	167	0.371	14	2336

12 days, 31 °C cm^{-1} gradient	<0.12	167	0.390	17	2836

The observed burial of bromide during the temperature gradient metamorphism may be attributed to a combination of growing ice, covering the bromide present at the air-ice interface with neat ice, and diffusion of the bromide into the growing ice as described in our previous work (Trachsel et al., 2019). Whether the bromide remains agglomerated forming micropockets under the growing ice, or forms a solid-solution in the growing ice remains somehow speculative. A recent study by Wu et al. (2017) showed that bromide is likely to be incorporated in the ice with recrystallization especially at low concentration. Molecular dynamics simulations by Wu et al. (2017) showed that the charge density around a bromide ion does not result in very large disruptions of the local ice structure. Therefore, they concluded that incorporating bromide into the ice structure may be energetically feasible. Patches at the interface may also be covered by the growing ice in line with Nagashima et al. (2018), who observed preferential growth of ice onto brine droplets compared to the neat ice surface.

The results presented here show that after 5 complete recrystallisation cycles the bromide is absent from the air-ice interface. This depletion of bromide at the air-ice interface is in excellent agreement with previous observations of other ions in snow during metamorphism (Hewitt et al., 1991; Cragin et al., 1996; Trachsel et al., 2019). Elution profiles of shock-frozen snow doped with a mixture of ammonium, calcium, chloride, fluoride, sodium, and sulphate revealed decreasing amounts of all ions at the air-ice interface with duration of snow metamorphism up to 12 days (Trachsel et al., 2019). On longer time scales, calcium and sulphate showed increasing occurrence at the air-ice interface. A further finding from Trachsel (2019) is that the cation and anion tend to experience the same fate in shock-frozen snow. One might thus speculate, that the sodium in the experiments presented here is likewise depleted at the air-ice interface during metamorphism. A more detailed and quantitative comparison with the elution studies is hampered, as the elution studies generally lack a budget of ions and give no direct link to chemical reactivity. Further, meltwater or the eluent, induce changes to the snow structure (wet metamorphism) and might lead to relocation of impurities (Meyer and Wania, 2008; Grannas et al., 2013).

1 Conclusion and Atmospheric Implication

We have presented an assessment of the effects of metamorphism on the loss of gas-phase ozone in bromide doped snow. Probing the presence of bromide in snow by its reaction with ozone is an effective way to reveal its location that is not amenable with other methods that would offer more chemical selectivity or spatial resolution but do lack sensitivity for the low impurity concentrations found in the environment. Experiments were performed in the dark in snow doped with 6.2 μM sodium bromide. The artificial snow had physical properties and a bromide concentration typical for natural snow, making extrapolations to the environment feasible. While snow is not formed by shock freezing in the environment, riming might occur and lead to similar distribution of impurities as observed in our samples. Further, we suggest that the patches of bromide at the air-ice interface

represent bromide that is deposited with sea salt aerosol on surface snow. Our observation of the ozone consumption showed that the bromide-doped snow samples lost their chemical reactivity towards gas-phase ozone during 12-days of temperature gradient metamorphism. This loss occurred without photochemistry forming volatile products. Post-depositional changes to bromide in snow have been observed in the field and have so far been explained by vivid photochemical reaction into volatile bromine. Volatile bromine might then be re-deposited on the snow surface after formation of more oxidized species, such as HOBr (Jacobi et al., 2002; Toom-Sauntry and Barrie, 2002). The burial of volatile trace gases into growing ice has also been discussed for acidic trace gases with atmospheric relevance (Huthwelker et al., 2006). Kippenberger et al. (2019) has studied the uptake of HCl and of oxidised organic trace gases to growing ice in Knudsen cell experiments. They observed a continuous uptake of HCl that exceeded the equilibrium partitioning of HCl to ice (Zimmermann et al., 2016) scaling with ice growth rate and temperature. Growth rates were varied between 2 nm s^{-1} and 110 nm s^{-1}. In this study, we uniquely show that non-volatile bromide ions are effectively buried. Apparently, temperature gradient metamorphism appears to facilitate the formation of energetically most favourable impurity distributions in snow.

Our findings directly imply that for the Earth surface snow, where temperature gradients are omnipresent, burial of non-volatile solutes during metamorphism can reduce their availability for heterogeneous reactions. That only a small fraction of impurities may be chemically active in surface snow has been discussed for nitrate by Thomas et al. (2011) and Wren and Donaldson (2011). Results from this study thus emphasize that the reactivity of impurities changes dramatically with time during temperature gradient metamorphism in the field, rather than being a result of the initial deposition process.

Clearly, the tendency to be incorporated into the ice matrix is a strong function of the chemical properties and of concentration (Bartels-Rausch et al., 2014; Trachsel et al., 2019). As a consequence, chemical species that were initially deposited together to the snow might separate to different compartments during metamorphism. The fact that bromide, for example, is driven into the ice while other potential reaction partners might leave the ice may lead to switching off other reaction pathways. For instance, the oxidation by OH radicals that are produced from organics ending up outside, too far away for the OH to reach the bromide.

We argued that the driving force for the relocation are temperature inhomogeneities and resulting water vapor fluxes, as frequently observed in surface snow. That ice is not in thermodynamic equilibrium is moreover a common situation for atmospheric ice particles as well with common sub- and super- saturation (Gao et al., 2004). Our results therefore suggest that similar re-distribution of ions might also occur prior to snowfall.

In the case of bromide, the re-distribution away from the interface will suppress an initiation step in bromine explosion and ozone depletion events, both in light and in the dark, even for snow samples that show high bromide concentrations. We propose that this finding -at least partially – explains the varying reactivity of Arctic surface snow. Pratt et al. (2013) has

investigated production of bromine for a range of saline snow and sea ice samples in outdoor chamber experiments and found no correlation with total bromide concentration in the samples and bromine release. It appeared that pristine snow, where the exchange with the atmosphere dominates its chemical composition, is more productive than snow that is in contact with sea water. Pratt et al. (2013) argued that deposition of atmospheric acids to the unbuffered surface snow drives the observed reactivity. Based on our finding, another explanation would be a constant flux of bromide from the atmosphere refurbishing the bromide that is buried by temperature gradient metamorphism and thus providing reactive bromide at the air-ice interface.

This finding has significant environmental implications as it does not only stress the importance of the location of chemical species on their reactivity, but shows that this location is rapidly changing in surface snow. One should note that incorporation of solutes into the interior of ice and snow makes them not only resistant to multiphase chemistry, but further reduces their tendency to be washed away by melt- or rain water percolating the snow. The enrichment in the snow may thus contribute to later release of toxins to the marine food web upon the complete melting of the snow (Wania et al., 1998; Eichler et al., 2001; Steffen et al., 2008; Durnford and Dastoor, 2011; Grannas et al., 2013). Further, even under current warming conditions the buried species might be promising candidate for reconstructing past atmospheric composition from ice core records that have experienced melt effects (Eichler et al., 2001).

1 Data availability

Edebeli, Jacinta; Bartels-Rausch, Thorsten (2020). Data set on bromide oxidation by ozone in snow during metamorphism from laboratory study. EnviDat. *doi:10.16904/envidat.138*.

1 Author Contribution

TB-R, AE, MS designed the MISO project that this study was part of. JE planned and performed the flow tube experiments with help and input from MA, AE, MS, SA, TB-R. JT and JE performed, analysed, and discussed the microCT measurements with input from MS. TB-R and JE analysed the ozone uptake data and wrote the manuscript with input from MA and all other authors. All authors approved the submitted version of the manuscript. This work is part of JE doctoral thesis at ETH Zürich.

1 Acknowledgement

Funding by the Swiss National Science Foundation (SNSF) under Grant No. 155999 is acknowledged. We thank Matthias Jaggi (SLF) and Mario Birrer (PSI) for their technical assistance, Margret Matzl (SLF) for her help in evaluating the microCT data.

References

Abbatt, J. P. D., Oldridge, N. W., Symington, A., Chukalovskiy, V., McWhinney, R. D., Sjostedt, S. J., and Cox, R. A.: Release of gas-phase halogens by photolytic generation of OH in frozen halide−nitrate solutions: An active halogen formation mechanism?, J. Phys. Chem. A, 114, 6527-6533, 10.1021/jp102072t, 2010.

Abbatt, J. P. D., Thomas, J. L., Abrahamsson, K., Boxe, C. S., Granfors, A., Jones, A. E., King, M. D., Saiz-Lopez, A., Shepson, P. B., Sodeau, J. R., Toohey, D. W., Toubin, C., von Glasow, R., Wren, S. N., and Yang, X.: Halogen activation via interactions with environmental ice and snow in the polar lower troposphere and other regions, Atmos. Chem. Phys., 12, 6237-6271, 10.5194/acp-12-6237-2012, 2012.

Artiglia, L., Edebeli, J., Orlando, F., Chen, S., Lee, M.-T., Corral Arroyo, P., Gilgen, A., Bartels-Rausch, T., Kleibert, A., Vazdar, M., Carignano, M. A., Francisco, J. S., Shepson, P. B., Gladich, I., and Ammann, M.: A surface-stabilized ozonide triggers bromide oxidation at the aqueous solution-vapour interface, Nat. Commun., 8, 700, 10.1038/s41467-017-00823-x, 2017.

Bartels-Rausch, T., Guimbaud, C., Gäggeler, H. W., and Ammann, M.: The partitioning of acetone to different types of ice and snow between 198 and 223 K, Geophys. Res. Lett., 31, L16110, 10.1029/2004gl020070, 2004.

Bartels-Rausch, T., Huthwelker, T., Gäggeler, H. W., and Ammann, M.: Atmospheric pressure coated-wall flow-tube study of acetone adsorption on ice, J. Phys. Chem. A, 109, 4531-4539, 10.1021/jp045187l, 2005.

Bartels-Rausch, T., Jacobi, H.-W., Kahan, T. F., Thomas, J. L., Thomson, E. S., Abbatt, J. P. D., Ammann, M., Blackford, J. R., Bluhm, H., Boxe, C. S., Dominé, F., Frey, M. M., Gladich, I., Guzman, M. I., Heger, D., Huthwelker, T., Klan, P., Kuhs, W. F., Kuo, M. H., Maus, S., Moussa, S. G., McNeill, V. F., Newberg, J. T., Pettersson, J. B. C., Roeselova, M., and Sodeau, J. R.: A review of air–ice chemical and physical interactions (AICI): Liquids, quasi-liquids, and solids in snow, Atmos. Chem. Phys., 14, 1587-1633, 10.5194/acp-14-1587-2014, 2014.

Bartels-Rausch, T., Orlando, F., Kong, X., Artiglia, L., and Ammann, M.: Experimental evidence for the formation of solvation shells by soluble species at a nonuniform air-ice interface, ACS Earth Space Chem., 1, 572-579, 10.1021/acsearthspacechem.7b00077, 2017.

Birkeland, K. W., Johnson, R. F., and Schmidt, S. D.: Near-surface faceted crystals formed by diurnal recrystallization: A case study of weak layer formation in the mountain snowpack and its contribution to snow avalanches, Arct. Alp. Res., 30, 200 - 204, 10.2307/1552135, 1998.

Blackford, J. R.: Sintering and microstructure of ice: A review, J. Phys. D: Appl. Phys., 40, R355-R385, 10.1088/0022-3727/40/21/R02, 2007.

Blackford, J. R., Jeffree, C. E., Noake, D. F. J., and Marmo, B. A.: Microstructural evolution in sintered ice particles containing NaCl observed by low-temperature scanning electron microscope, Proc. Inst. Mech. Eng, 221, 151-156, 10.1243/14644207JMDA134, 2007.

Calonne, N., Geindreau, C., Flin, F., Morin, S., Lesaffre, B., Rolland du Roscoat, S., and Charrier, P.: 3-d image-based numerical computations of snow permeability: Links to specific surface area, density, and microstructural anisotropy, Cryosphere, 6, 939-951, 10.5194/tc-6-939-2012, 2012.

Cragin, J. H., Hewitt, A. D., and Colbeck, S. C.: Grain-scale mechanisms influencing the elution of ions from snow, Atmos. Environ., 30, 119-127, 10.1016/1352-2310(95)00232-N, 1996.

Crowley, J. N., Ammann, M., Cox, R. A., Hynes, R. G., Jenkin, M. E., Mellouki, A., Rossi, M. J., Troe, J., and Wallington, T. J.: Evaluated kinetic and photochemical data for atmospheric chemistry: Volume V – heterogeneous reactions on solid substrates, Atmos. Chem. Phys., 10, 9059-9223, 10.5194/acp-10-9059-2010, 2010.

Dominé, F., and Rey-Hanot, L.: Adsorption isotherms of acetone on ice between 193 and 213 K, Geophys. Res. Lett., 29, 1873, 10.1029/2002GL015078, 2002.

Dominé, F., and Shepson, P. B.: Air-snow interactions and atmospheric chemistry, Science, 297, 1506-1510, 10.1126/science.1074610, 2002.

Dominé, F., Albert, M. R., Huthwelker, T., Jacobi, H.-W., Kokhanovsky, A. A., Lehning, M., Picard, G., and Simpson, W. R.: Snow physics as relevant to snow photochemistry, Atmos. Chem. Phys., 8, 171-208, 10.5194/acp-8-171-2008, 2008.

Dominé, F., Barrere, M., Sarrazin, D., Morin, S., and Arnaud, L.: Automatic monitoring of the effective thermal conductivity of snow in a low-arctic shrub tundra, Cryosphere, 9, 1265-1276, 10.5194/tc-9-1265-2015, 2015.

Durnford, D., and Dastoor, A.: The behavior of mercury in the cryosphere: A review of what we know from observations, J. Geophys. Res., 116, 10.1029/2010jd014809, 2011.

Ebner, P. P., Steen-Larsen, H. C., Stenni, B., Schneebeli, M., and Steinfeld, A.: Experimental observation of transient δ18o interaction between snow and advective airflow under various temperature gradient conditions, Cryosphere, 11, 1733-1743, 10.5194/tc-11-1733-2017, 2017.

Edebeli, J., Ammann, M., and Bartels-Rausch, T.: Microphysics of the aqueous bulk counters the water activity driven rate acceleration of bromide oxidation by ozone from 289–245 K, Environ Sci Process Impacts, 21, 63-73, 10.1039/c8em00417j, 2019.

Eichler, A., Schwikowski, M., and Gäggeler, H. W.: Meltwater-induced relocation of chemical species in alpine firn, Tellus B, 53, 192-203, DOI 10.1034/j.1600-0889.2001.d01-15.x, 2001.

Gao, R. S., Fahey, D. W., Kärcher, B., and Peter, T.: Evidence that nitric acid increases relative humidity in low-temperature cirrus clouds, Science, 303, 516-520, 10.1126/science.1091255, 2004.

Grannas, A. M., Bogdal, C., Hageman, K. J., Halsall, C., Harner, T., Hung, H., Kallenborn, R., Klán, P., Klánová, J., Macdonald, R. W., Meyer, T., and Wania, F.: The role of the global cryosphere in the fate of organic contaminants, Atmos. Chem. Phys., 13, 3271-3305, 10.5194/acp-13-3271-2013, 2013.
Haag, W. R., and Hoigne, J.: Ozonation of bromide-containing waters: Kinetics of formation of hypobromous acid and bromate, Environ. Sci. Technol., 17, 261-267, 10.1021/es00111a004, 1983.
Hagenmuller, P., Chambon, G., Flin, F., Morin, S., and Naaim, M.: Snow as a granular material: Assessment of a new grain segmentation algorithm, Granular Matter, 16, 421-432, 10.1007/s10035-014-0503-7, 2014.
Hagenmuller, P., Flin, F., Dumont, M., Tuzet, F., Peinke, I., Lapalus, P., Dufour, A., Roulle, J., Pézard, L., Voisin, D., Ando, E., Rolland du Roscoat, S., and Charrier, P.: Motion of dust particles in dry snow under temperature gradient metamorphism, Cryosphere, 13, 2345-2359, 10.5194/tc-13-2345-2019, 2019.
Heeb, M. B., Criquet, J., Zimmermann-Steffens, S. G., and von Gunten, U.: Oxidative treatment of bromide-containing waters: Formation of bromine and its reactions with inorganic and organic compounds - a critical review, Water Res, 48, 15-42, 10.1016/j.watres.2013.08.030, 2014.
Hewitt, A. D., Cragin, J. H., and Colbeck, S. C.: Does snow have ion chromatographic properties?, 46th Ann. Eastern Snow Conference, Quebec City, Quebec, Canada, 1989, 165-171,
Hewitt, A. D., Cragin, J. H., and Colbeck, S. C.: Effects of crystal metamorphosis on the elution from chemical species from snow, 48th Ann. Eastern Snow Conference, Guelph, Ontario, Canada, 1991, 1-10,
Hullar, T., and Anastasio, C.: Direct visualization of solute locations in laboratory ice samples, Cryosphere, 10, 2057-2068, 10.5194/tc-10-2057-2016, 2016.
Huthwelker, T., Ammann, M., and Peter, T.: The uptake of acidic gases on ice, Chem. Rev., 106, 1375-1444, 10.1021/Cr020506v, 2006.
Jacobi, H.-W., Frey, M. M., Hutterli, M. A., Bales, R. C., Schrems, O., Cullen, N. J., Steffen, K., and Koehler, C.: Measurements of hydrogen peroxide and formaldehyde exchange between the atmosphere and surface snow at Summit, Greenland, Atmos. Environ., 36, 2619-2628, 10.1016/S1352-2310(02)00106-1, 2002.
Jacobi, H.-W., Voisin, D., Jaffrezo, J. L., Cozic, J., and Douglas, T. A.: Chemical composition of the snowpack during the OASIS spring campaign 2009 at Barrow, Alaska, J. Geophys. Res., 117, D00R13-n/a, 10.1029/2011JD016654, 2012.
Kämpfer, T. U., Schneebeli, M., and Sokratov, S. A.: A microstructural approach to model heat transfer in snow, Geophys. Res. Lett., 32, L21503, 10.1029/2005GL023873, 2005.
Kärcher, B., and Basko, M. M.: Trapping of trace gases in growing ice crystals, J. Geophys. Res., 109, D22204, 10.1029/2004JD005254, 2004.
Kerbrat, M., Huthwelker, T., Gäggeler, H. W., Ammann, M., and Schneebeli, M.: Measuring the specific surface area of snow with X-ray tomography and gas adsorption: Comparison and implications for surface smoothness, Atmos. Chem. Phys., 8, 1261-1275, 10.5194/acp-8-1261-2008, 2008.
Kippenberger, M., Schuster, G., Lelieveld, J., and Crowley, J. N.: Trapping of HCl and oxidised organic trace gases in growing ice at temperatures relevant to cirrus clouds, Atmos. Chem. Phys., 19, 11939-11951, 10.5194/acp-19-11939-2019, 2019.
Kong, X., Waldner, A., Orlando, F., Artiglia, L., Huthwelker, T., Ammann, M., and Bartels-Rausch, T.: Coexistence of physisorbed and solvated HCl at warm ice surfaces, J. Phys. Chem. Lett., 8, 4757-4762, 10.1021/acs.jpclett.7b01573, 2017.
Krepelova, A., Bartels-Rausch, T., Brown, M. A., Bluhm, H., and Ammann, M.: Adsorption of acetic acid on ice studied by ambient-pressure XPS and partial-electron-yield NEXAFS spectroscopy at 230–240 K, J. Phys. Chem. A, 117, 401-409, 10.1021/jp3102332, 2013.
Langenberg, S., and Schurath, U.: Ozone destruction on ice, Geophys. Res. Lett., 26, 1695-1698, 10.1029/1999gl900325, 1999.
Legagneux, L., Cabanes, A., and Dominé, F.: Measurement of the specific surface area of 176 snow samples using methane adsorption at 77 K, J. Geophys. Res., 107, 4335, 10.1029/2001JD001016, 2002.
Löwe, H., Spiegel, J. K., and Schneebeli, M.: Interfacial and structural relaxations of snow under isothermal conditions, J. Glaciol., 57, 499-510, 10.3189/002214311796905569, 2011.
McFall, A. S., Edwards, K. C., and Anastasio, C.: Nitrate photochemistry at the air-ice interface and in other ice reservoirs, Environ. Sci. Technol., 52, 5710-5717, 10.1021/j.acs.est.8b00095, 2018.
Meyer, T., and Wania, F.: Organic contaminant amplification during snowmelt, Water Research, 42, 1847-1865, 10.1016/j.watres.2007.12.016, 2008.
Nagashima, K., Sazaki, G., Hama, T., Murata, K.-i., and Furukawa, Y.: Uptake mechanism of atmospheric hydrogen chloride gas in ice crystals via hydrochloric acid droplets, Crystal Growth & Design, 18, 4117-4122, 10.1021/acs.cgd.8b00531, 2018.
Oldridge, N. W., and Abbatt, J. P. D.: Formation of gas-phase bromine from interaction of ozone with frozen and liquid NaCl/NaBr solutions: Quantitative separation of surficial chemistry from bulk-phase reaction, J. Phys. Chem. A, 115, 2590-2598, 10.1021/jp200074u, 2011.
Peybernes, N., Marchand, C., Le Calve, S., and Mirabel, P.: Adsorption studies of acetone and 2,3-butanedione on ice surfaces between 193 and 223 K, Phys. Chem. Chem. Phys., 6, 1277-1284, 10.1039/b315064j, 2004.
Pinzer, B., and Schneebeli, M.: Breeding snow: An instrumented sample holder for simultaneous tomographic and thermal studies, Meas. Sci. Technol., 20, 10.1088/0957-0233/20/9/095705, 2009.

Pinzer, B. R., Schneebeli, M., and Kämpfer, T. U.: Vapor flux and recrystallization during dry snow metamorphism under a steady temperature gradient as observed by time-lapse micro-tomography, Cryosphere, 6, 1141-1155, 10.5194/tc-6-1141-2012, 2012.
Pratt, K. A., Custard, K. D., Shepson, P. B., Douglas, T. A., Pöhler, D., General, S., Zielcke, J., Simpson, W. R., Platt, U., Tanner, D. J., Gregory Huey, L., Carlsen, M., and Stirm, B. H.: Photochemical production of molecular bromine in arctic surface snowpacks, Nat. Geosi., 6, 351-356, 10.1038/ngeo1779, 2013.
Riche, F., Bartels-Rausch, T., Schreiber, S., Ammann, M., and Schneebeli, M.: Temporal evolution of surface and grain boundary area in artificial ice beads and implications for snow chemistry, J. Glaciol., 58, 815-817, 10.3189/2012JoG12J058, 2012.
Rumble, J.: CRC handbook of chemistry and physics, 100th edition, in, CRC Press, 2019.
Saiz-Lopez, A., and von Glasow, R.: Reactive halogen chemistry in the troposphere, Chem. Soc. Rev., 41, 6448-6472, 10.1039/C2CS35208G, 2012.
Schmidt, J. A., Jacob, D., Horowitz, H. M., Hu, L., Sherwen, T., Evans, M. J., Liang, Q., Suleiman, R. M., Oram, D. E., Le Breton, M., Percival, C. J., Wang, S., Dix, B., and Volkamer, R.: Modeling the observed tropospheric BrO background: Importance of multiphase chemistry and implications for ozone, OH, and mercury, J. Geophys. Res., 121, 11819-11835, 10.1002/2015JD024229, 2016.
Schweizer, J.: Snow and avalanche research: A journey across scales, Cold Reg. Sci. Technol., 108, 69-71, 10.1016/j.coldregions.2014.09.011, 2014.
Simpson, W. R., von Glasow, R., Riedel, K., Anderson, P., Ariya, P., Bottenheim, J., Burrows, J., Carpenter, L. J., Friess, U., Goodsite, M. E., Heard, D., Hutterli, M., Jacobi, H. W., Kaleschke, L., Neff, B., Plane, J., Platt, U., Richter, A., Roscoe, H., Sander, R., Shepson, P., Sodeau, J., Steffen, A., Wagner, T., and Wolff, E.: Halogens and their role in polar boundary-layer ozone depletion, Atmos. Chem. Phys., 7, 4375-4418, 10.5194/acp-7-4375-2007, 2007.
Simpson, W. R., Brown, S. S., Saiz-Lopez, A., Thornton, J. A., and von Glasow, R.: Tropospheric halogen chemistry: Sources, cycling, and impacts, Chem. Rev., 115, 4035-4062, 10.1021/cr5006638, 2015.
Steen-Larsen, H. C., Johnsen, S. J., Masson-Delmotte, V., Stenni, B., Risi, C., Sodemann, H., Balslev-Clausen, D., Blunier, T., Dahl-Jensen, D., Ellehøj, M. D., Falourd, S., Grindsted, A., Gkinis, V., Jouzel, J., Pope, F. D., Sheldon, S., Simonsen, S. B., Sjolte, J., Steffensen, J. P., Sperlich, P., Sveinbjörnsdóttir, A. E., Vinther, B. M., and White, J. W. C.: Continuous monitoring of summer surface water vapor isotopic composition above the Greenland ice sheet, Atmos. Chem. Phys., 13, 4815-4828, 10.5194/acp-13-4815-2013, 2013.
Steen-Larsen, H. C., Masson-Delmotte, V., Hirabayashi, M., Winkler, R., Satow, K., Prié, F., Bayou, N., Brun, E., Cuffey, K. M., Dahl-Jensen, D., Dumont, M., Guillevic, M., Kipfstuhl, S., Landais, A., Pope, F. D., Risi, C., Steffen, K., Stenni, B., and Sveinbjörnsdóttir, A. E.: What controls the isotopic composition of Greenland surface snow?, Cryosphere, 10, 377-392, 2014.
Steffen, A., Douglas, T. A., Amyot, M., Ariya, P. A., Aspmo, K., Aspmo, K., Berg, T., Bottenheim, J. W., Brooks, S., Cobbett, F., Dastoor, A. P., Dommergue, A., Ebinghaus, R., Ferrari, C., Gardfeldt, K., Goodsite, M. E., Lean, D., Poulain, A. J., Scherz, C., Skov, H., Sommar, J., and Temme, C.: A synthesis of atmospheric mercury depletion event chemistry in the atmosphere and snow, Atmos. Chem. Phys., 8, 1445-1482, 10.5194/acp-8-1445-2008, 2008.
Stephen, H., and Stephen, T.: Solubility of various compounds in water, in: Binary systems, edited by: Stephen, H., and Stephen, T., Pergamon, 5-960, 1963.
Thibert, E., and Dominé, F.: Thermodynamics and kinetics of the solid solution of HCl in ice, J. Phys. Chem. B, 101, 3554-3565, 10.1021/jp962115o, 1997.
Thibert, E., and Dominé, F.: Thermodynamics and kinetics of the solid solution of HNO3 in ice, J. Phys. Chem. B, 102, 4432-4439, 10.1021/jp980569a, 1998.
Thomas, J. L., Stutz, J., Lefer, B., Huey, L. G., Toyota, K., Dibb, J. E., and von Glasow, R.: Modeling chemistry in and above snow at Summit, Greenland – part 1: Model description and results, Atmos. Chem. Phys., 11, 4899-4914, 10.5194/acp-11-4899-2011, 2011.
Toom-Sauntry, D., and Barrie, L. A.: Chemical composition of snowfall in the high arctic: 1990–1994, Atmos. Environ., 36, 2683-2693, 10.1016/S1352-2310(02)00115-2, 2002.
Trachsel, J. C., Avak, S. E., Edebeli, J., Schneebeli, M., Bartels-Rausch, T., Bruetsch, S., and Eichler, A.: Microscale rearrangement of ammonium induced by snow metamorphism, Front. Earth Sci., 7, 10.3389/feart.2019.00194, 2019.
Ullerstam, M., and Abbatt, J. P. D.: Burial of gas-phase HNO3 by growing ice surfaces under tropospheric conditions, Phys. Chem. Chem. Phys., 7, 3596-3600, 10.1039/b507797d, 2005.
Waldner, A., Artiglia, L., Kong, X., Orlando, F., Huthwelker, T., Ammann, M., and Bartels-Rausch, T.: Pre-melting and the adsorption of formic acid at the air–ice interface at 253 K as seen by NEXAFS and XPS, Phys. Chem. Chem. Phys., 20, 24408-24417, 10.1039/C8CP03621G, 2018.
Wania, F., Hoff, J. T., Jia, C. Q., and Mackay, D.: The effects of snow and ice on the environmental behaviour of hydrophobic organic chemicals, Environ. Pollut., 102, 25-41, 10.1016/S0269-7491(98)00073-6, 1998.
Winkler, A. K., Holmes, N. S., and Crowley, J. N.: Interaction of methanol, acetone and formaldehyde with ice surfaces between 198 and 223 K, Phys. Chem. Chem. Phys., 4, 5270-5275, 10.1039/b206258e, 2002.
Wren, S. N., Kahan, T. F., Jumaa, K. B., and Donaldson, D. J.: Spectroscopic studies of the heterogeneous reaction between O3(g) and halides at the surface of frozen salt solutions, J. Geophys. Res., 115, 660, 10.1029/2010JD013929, 2010.

Wren, S. N., and Donaldson, D. J.: Exclusion of nitrate to the air-ice interface during freezing, J. Phys. Chem. Lett., 2, 1967-1971, 10.1021/Jz2007484, 2011.
Wren, S. N., Donaldson, D. J., and Abbatt, J. P. D.: Photochemical chlorine and bromine activation from artificial saline snow, Atmos. Chem. Phys., 13, 9789-9800, 10.5194/acp-13-9789-2013, 2013.
Wu, S., Zhu, C., He, Z., Xue, H., Fan, Q., Song, Y., Francisco, J. S., Zeng, X. C., and Wang, J.: Ion-specific ice recrystallization provides a facile approach for the fabrication of porous materials, Nat. Commun., 8, 1-8, 10.1038/ncomms15154, 2017.
Zermatten, E., Haussener, S., Schneebeli, M., and Steinfeld, A.: Tomography-based determination of permeability and dupit-forchheimer coefficient of characteristic snow samples, J. Glaciol., 57, 811-816, 2011.
Zimmermann, S., Kippenberger, M., Schuster, G., and Crowley, J. N.: Adsorption isotherms for hydrogen chloride (HCl) on ice surfaces between 190 and 220 K, Phys. Chem. Chem. Phys., 18, 13799-13810, 10.1039/C6CP01962E, 2016.